Available online at www.sciencedirect.com

SciVerse ScienceDirect

Procedia Environmental Sciences 19 (2013) 416 – 425

Procedia
Environmental Sciences

Four Decades of Progress in Monitoring and Modeling Processes in the Soil-Plant-Atmosphere System: Applications and Challenges

Use of a fractional brownian motion model to mimic spatial horizontal variation of soil physical and hydraulic properties displaying a power-law variogram

A. Comegna[a*], A. Coppola[b], V. Comegna[a], A. Sommella[c], C.D. Vitale[d]

[a]*School of Agricultural Forestry Food and Environmental Sciences (SAFE), University of Basilicata, Potenza, Italy, (email: alessandro.comegna@unibas.it).*
[b]*Department of European and Mediterranean Cultures-Architecture, Environment, Cultural Heritage (DiCEM), Hydraulics and Hydrology Division, University of Basilicata, Matera, Italy.*

[c]*Division of Water Resources Management, University of Naples "Federico II", Italy*

[d] *Department of Economics and Statistical Science, University of Salerno (Italy)*

Abstract

Stochastic analysis of flow and mass transport in soil, usually assumes that soil hydraulic properties are stationary homogeneous stochastic processes with a finite variance. Some field data suggest that soil hydraulic distributions may have a fractal character with long-range correlations. In this study new field soil hydraulic data-sets, measured along transects of an Andosol and a Vertic-Fluvent soil, were analyzed for fractal behavior using a stochastic fractal function such as fractional Brownian motion (fBm) and power-law variogram fits to estimate the monofractal Hurst exponent H as a measure of self-similarity. Our analysis lend further support to the hypothesis that horizontal processes, that mimic fBm, will display a power-law variogram.

Selection and/or peer-review under responsibility of the Scientific Committee of the conference

Keywords: Horizontal soil heterogeneity, fractional Brownian model (fBm), fractal dimension.

1. Introduction

Many phenomena studied in geology show notable properties of scale invariance. Fragmentation processes of the Earth's crust, for example, occur with similar mechanisms at very different scales [1]. By

* Corresponding author. Tel.: +39-0971-102-474
E-mail address: alessandro.comegna@unibas.it

1878-0296
Selection and/or peer-review under responsibility of the Scientific Committee of the Conference
doi:10.1016/j.proenv.2013.06.048

the same token, the structure of drainage networks and rainfall essentially stays the same regardless of the scale of observation in question [2].

This consideration, at times formalized mathematically by widely accepted empirical laws, has recently given rise to renewed interest, essentially due to the impulse given by the works of Mandelbrot [3] on fractal geometry to geophysics and hydrology. This tool is particularly suited to describing the disorder of natural objects. However, this disorder often possesses a certain structure or internal coherence: without an appropriate reference it is difficult, for each of the cases cited, to understand the scale of observation from a photograph. This characteristic, thanks to which an object observed at different scales always shows the same appearance, is called *self-similarity* or *scale invariance*.

Fractal geometry is effective at describing such objects that have a dimension which, unlike what happens in Euclidean geometry, is not an *integer*.

Analysis of natural geometries in terms of *invariant-scale* structures or *fractals* is assuming ever-increasing importance in the study of spatial variability, in measuring soil aggregates, size of soil particles [5] and soil hydraulic properties [6; 7; 4].

Initial research in this area did not consider the spatial structure of soil hydraulic properties, assuming that they behave like a *white noise* process [8]. Later research considered spatial correlation of flow properties. Various autocovariance functions, including anisotropic ones, were used to describe the spatial correlation [9; 10; 11; 12; 13; 14; 15; 16]. However, in most such efforts it was assumed that the correlation structure of parameter fluctuations is such that the fluctuation variance is bounded and reaches its asymptotic value as the volume of the analysed region increases. The validity of this assumption for geological formations has yet to be demonstrated. The field data from the rather homogeneous *Border* site [17] indicate that, at least for this site, the assumption is valid. Other sites, however, show *scale-dependent* variance and *long-range* correlations of soil hydraulic properties [18; 19; 20]. This dependence on scale is amply illustrated by Gajem [21] who examined a region of 85 ha at three sampling scales on a transect at 0.20, 1.00, 20.00 m intervals, increasing transect lengths in proportion. As the length of the transects increased, so did the variance and the range of dependence.

Such facts led us to consider whether some soil properties, in particular pedological contexts in southern Italy, exhibited *true similarity* at different scales [19] and to explore its representation by fractals [3]. We will take as a starting point the stochastic fractal of linear Brownian motion (fBm) which began to be applied in Soil Hydrology during the early 1900’s [22]. Numerous additional applications followed [23]

2. Fractional Brownian motion (fBm)

Process $Y(x)$ is termed *Brownian* if:

$$Y(x+h) = Y(x) - \varepsilon(x,h) \tag{1}$$

where $\varepsilon(x,h)$ is a stochastic Gaussian process with zero constant mean and variance equal to *h*, independent of *x*. The variogram of *Y* coincides with the variance of $\varepsilon(x,h)$ and is:

$$\gamma(h) = E\big[Y(x+h) - Y(x)\big]^2 = E\big[\varepsilon(x,h)\big]^2 = \mathrm{var}\big[\varepsilon(x,h)\big] = h^{2H} \tag{2}$$

where *H* is the *Hurst* exponent [24], a real number with values between $0 < H < 1$. If the sampling interval is divided by any arbitrary positive value *r* and the result rescaled in the ratio r^H, then the new semivariogram will be identical to the old one. In this sense Brownian motion is a *self-similar* or *fractal process*.

In ordinary Brownian motion the successive values of ε are totally independent. The generalisation proposed by Mandelbrot and Wallis [25], for $0 < H < 1$, defines a fractional Brownian process whose irregularity is a function of *H*. In particular, for *H=0* the process $\varepsilon(x,h)$ is reduced to classical *white noise* and $Y(x)$ to the well-known *random walk*, and for *H=1* the process $Y(x)$ becomes *smooth*. Figure 1 reports some realisations of $Y(x)$ at different *H* values.

A further generalisation of this fractional Brownian process, in the case of a discrete h, was proposed in Mandelbrot [26]. This generalisation was obtained by making $\varepsilon(x,h)$ a Gaussian process with zero mean and unit variance, but with an autocovariance function given by

$$C(h, H) = \frac{1}{2}\left[|h+1|^{2H} - 2|h|^{2H} + |h-1|^{2H}\right] \tag{3}$$

where h is the spatial or temporal *lag*, while $0 < H < 1$. It can be easily proved that when *H*=0 or *H*=0.5, then $\varepsilon(x,h)$ becomes the classic normal *white noise* process, while for *H*>0.5 the function *C*(*h, H*) is always positive. Hence positive values of $\varepsilon(x,h)$ tend to be followed by positive values and the same occurs for negative values (*persistence*). Therefore the closer *H* is to one, the smoother the process becomes. For 0<*H*<0.5 the autocovariance function of $\varepsilon(x,h)$ is negative and hence with positive values of $\varepsilon(x,h)$ there tend to be negative values, and vice versa, and the relative stochastic process is very noisy. For both the above processes, it may be demonstrated [27] that their normal *Hausdorff-Besicowitch* fractal dimension *D* is a simple function of *H* given by

$$2H = 4 - 2D \tag{4}$$

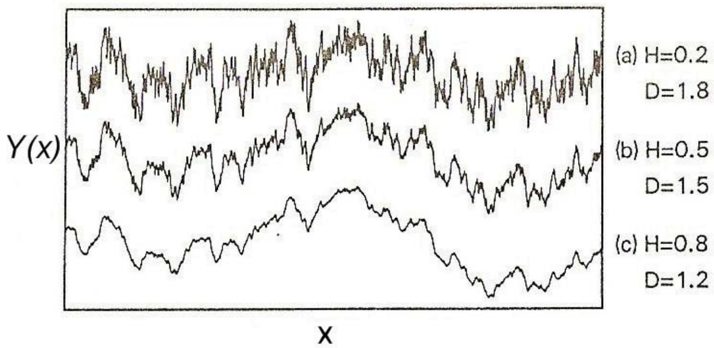

Figure 1. Realizations of the stochastic process *Y(x)*, for different values of *H*.

which according to Mandelbrot [3] exceed the topological dimension. Barry and Lewis [28] showed that equation (4) also holds good for another fractal process, that of *Weierstrass-Mandeltrot*. Such considerations lead us to believe that model (2) is fairly general to obtain an acceptable estimate of *D*. Taking logarithms of both sides of equation (2) the following linear equation is obtained:

$$\log(\gamma(h)) = 2H \log(h) \tag{5}$$

with a linear coefficient equal to $2H$, which allows an estimate of $2H$ to be obtained with the classic least squares method, estimating $\gamma(h)$ from observed data and then interpolating the straight line (equation 5) with zero intercept. Having estimated H, by means of (4) we obtain straightaway an estimate of D:

$$D = \frac{4 - 2H}{2} \tag{6}$$

Physical interpretation of the fractal dimension D is fairly simple: the closer D is to *1* the closer we are to the linear *smooth* case. Conversely, the closer D is to *2*, the closer we are to the classic *random walk* process, and hence erratic and hard to predict.

3. An application on Andosol and Vertic Fluvent soils

The Brownian model was applied to several series of data, observed at constant distance, along transects of the type shown in figure 2:

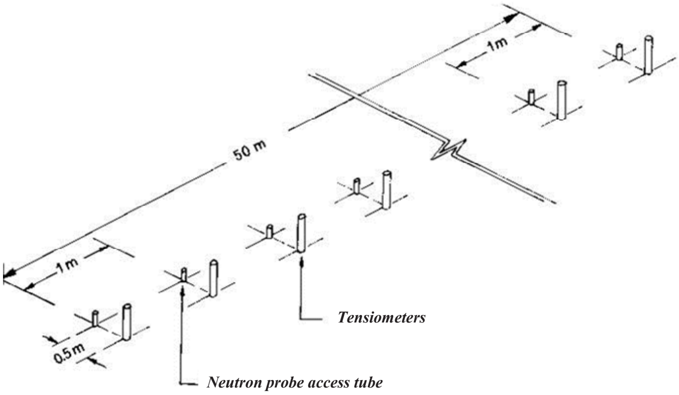

Figure 2. A schematic representation of the experimental transects.

The analyzed series refer to particular values of i) volumetric water content of soil θ, ii) water potential p/γ (cm), iii) water flux density q (cm/h), iv) water storage S (mm), v) clay content AG (%); vi) temperature TMP (°C). These series are presented in detail below.

3.1. Series observed on an Andosol in a plot at Ponticelli (Naples)

- Series θ_l , $l=1, 2, ..., 50m$, obtained by measuring water content with a neutron probe, at 48 hours from the start of a drainage test with soil surface evaporation prevented.

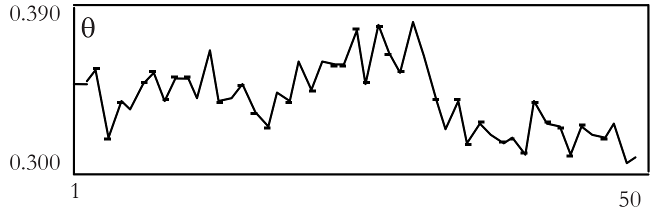

- Series $\left(\frac{p}{\gamma}\right)_l$, *l = 1, 2, ..., 50m*, obtained by measuring water potential with mercury tensiometers, at *312* h from the start of drainage.

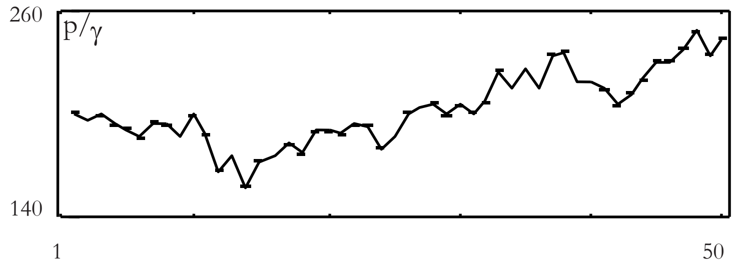

- Series q_l, *l=1, 2, ..., 50m*, obtained by using Darcy's Law to calculate the water flux density within the soil profile for *t=48* h and *z = 90 cm*.

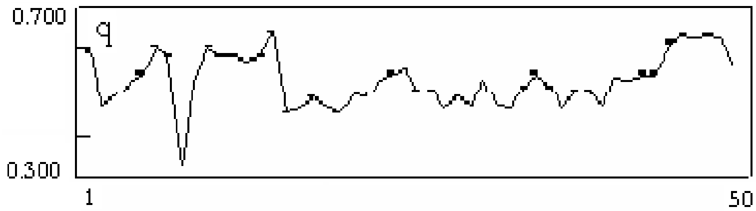

- Series S_l, *l=1, 2, ..., 50m*, obtained in the presence of a major winter crop, numerically integrating water content profiles to a depth of *90 cm*.

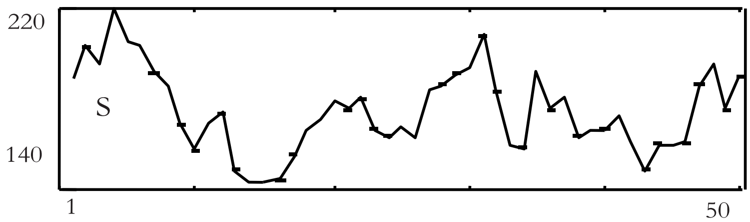

- Series AG_l, *l =1, 2, ..., 50m*, obtained by measuring, for *z=30cm*, the percentage content of clay in the soil.

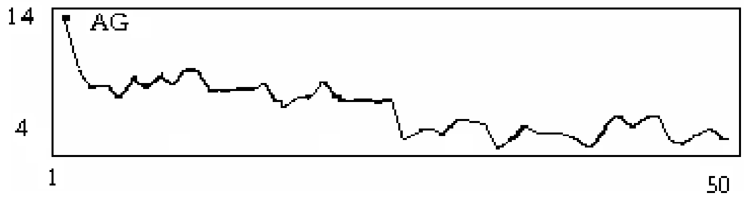

3.2. Series observed on a Vertic-Fluvent soil in a plot at Policoro (MT)

- Series θ_l, l=*1, 2, ..., 132*, obtained by measuring soil volumetric water content at an interaxis distance of *0.25m* between the rows of a pepper crop after irrigation supply of about *400 m³/ha*.

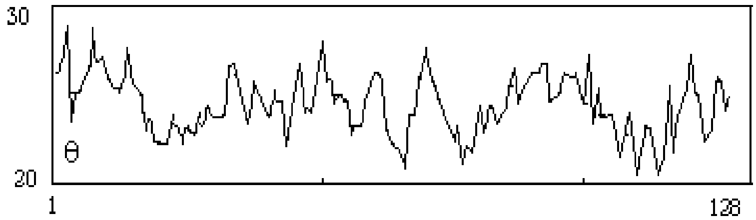

- Series TMP_l, *l =1, 2, ..., 132*, at the measuring points of the previous series, with an infrared thermometer (mod. *Campbell PRT5* sensitive to wavelengths of *8-14μ* ; under a viewing angle of *8°* it observes a field of *6.5cm²*).
-

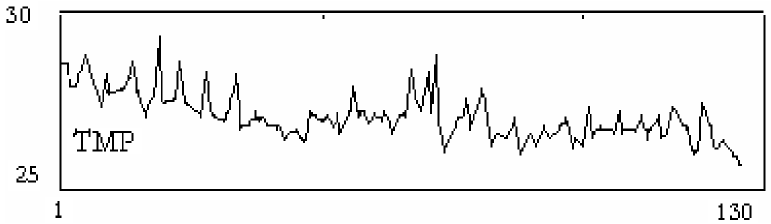

4. Results and Discussion

For the above series, the relevant variograms are reported below (figures 3-9).

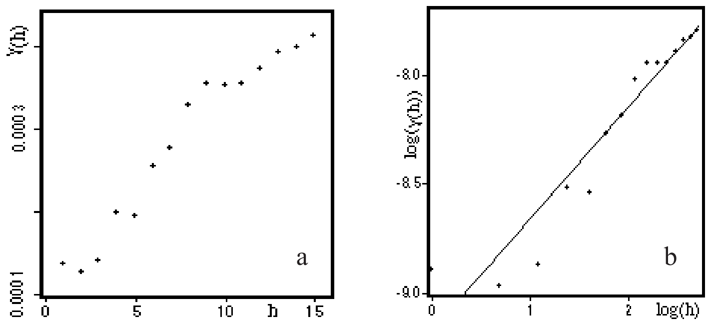

Figure 3 (a) Empirical variogram for θ on Andosol; (b) Logarithmic plot of empirical variogram and relative fitting curve.

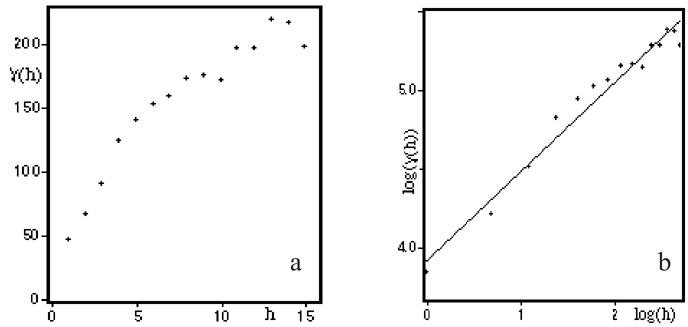

Figure 4 (a) Empirical variogram for p/γ on Andosol; (b) Logarithmic plot of empirical variogram and relative fitting curve.

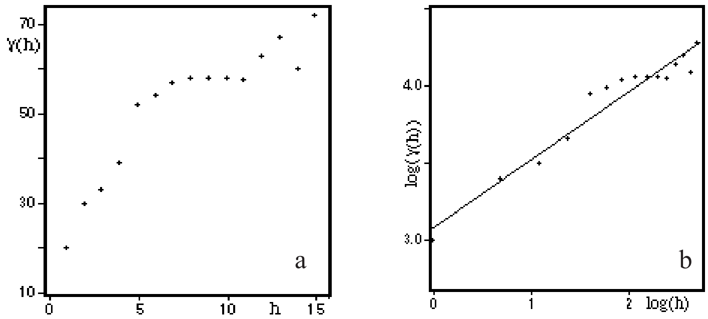

Fig. 5 (a) Empirical variogram for q on Andosol; (b) Logarithmic plot of empirical variogram and relative fitting curve.

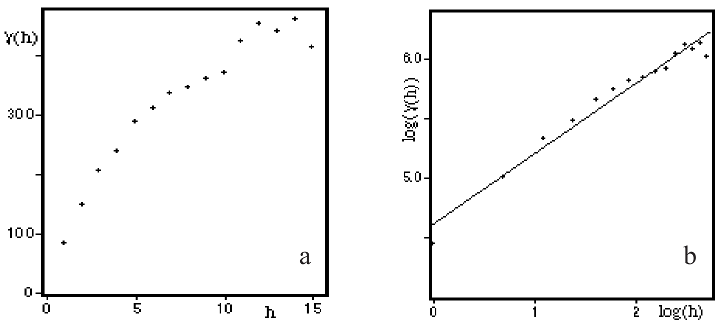

Fig. 6 (a) Empirical variogram for S on Andosol; (b) Logarithmic plot of empirical variogram and relative fitting curve.

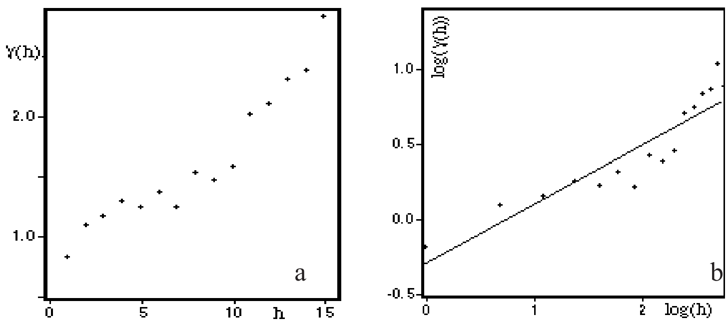

Fig. 7 (a) Empirical variogram for AG on Andosol; (b) Logarithmic plot of empirical variogram and relative fitting curve.

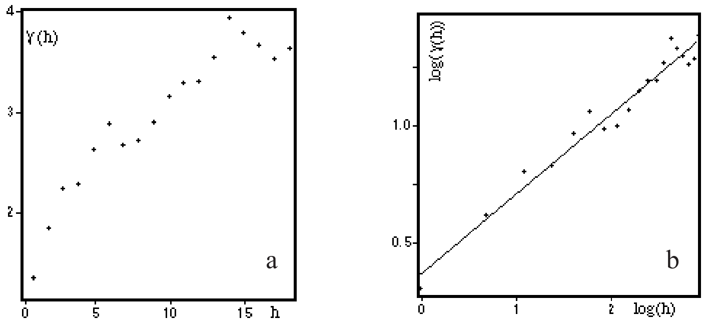

Fig. 8 (a) Empirical variogram for θ on Fluvent soil; (b) Logarithmic plot of empirical variogram and relative fitting curve.

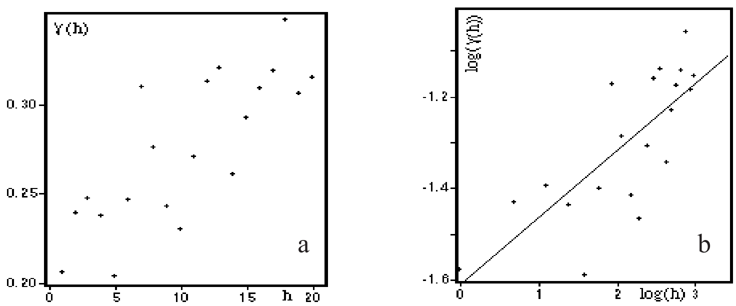

Fig. 9 (a) Empirical variogram for TMP on Fluvent soil; (b) Logarithmic plot of empirical variogram and relative fitting curve.

Examination of the variograms of the Andosol series (figure 3a-7a) shows that they have a similar form, which indicates that, despite the difference in mean transect levels, their spatial structure is similar.

Vice versa, the variogram of the Vertic soil (8a-9a), being the product of a process with rather weak correlations, is flat and less interpretable in terms of *nugget* variance.

Estimation of the fractal dimensions of the series was then simply inferred from the variograms in figures 3b-9b whose slope, as shown in the section above, is equal to *4-2D*. Estimation of the slope for the first *15–20 lags* of the variograms was performed with the least squares method. Such estimates are reported in table 1 which supplies other information on the structure of the series examined: soil type, variable type, spatial-*lag*, goodness of fit index (R^2) of the variograms observed on double logarithmic scale.

Tab. 1 - Estimate of fractal dimensions of the seven series examined and goodness of fit index R^2

Soil	Parameters	Lag (m)	D	R^2
Andosol	θ	1.00	1.74	0.91
Andosol	p/γ	1.00	1.72	0.97
Andosol	q	1.00	1.78	0.94
Andosol	S	1.00	1.70	0.97
Andosol	AG	1.00	1.80	0.82
Vertic-Fluent	θ	0.25	1.83	0.96
Vertic-Fluent	TMP	0.25	1.93	0.58

From the results obtained, it may be noted that the fractal dimension lies in the interval (1.7-2.0). In particular, it must be observed, for the *TMP* series, the highest value for *D* at the lowest goodness index of fit R^2=0.58. This result may be explained by the fact that this series is coloured by the instrumental noise of the thermometer used which was able to modify the measurement of the parameter in question to such an extent as to mask self-similarity substantially. In general, the values estimated for all the other series are compatible with those published in the international literature [3; 29; 30], confirming that soils may vary more randomly than Brownian motion. It may be assumed that the different, independent factors, that affect the variation of the series combine with one another to mask the fractal property of statistical self-similarity at all scales.

5. Conclusions

The horizontal spatial variability of some soil hydraulic properties measured along transects by non destructive techniques, was analyzed using a fractional Brownian motion (fBm) model. In the special case of the scale-invariant distributions observed on an Andosol and on a Vertic-Fluvent soil, the scaling monofractal Hurst exponent has been obtained from log-log plots of $\gamma(h)$ vs *h* and used as a measured of self-similarity. The values of *H* lay between *0.0* and *0.5*, and thus the fractal dimension *D* lay between *1.7* and *2.0* suggesting that soil varied more randomly than Brownian motion. While this may be so, we concluded that various independent factors that affect soil variation combined in a way that can overshadow self-similarity. Nevertheless the fractal representation should be borne in mind by soil hydrologists and D values of soil properties computed for reference against those of Brownian fractals.

There is further to understand the physical interpretation of fractal dimension and to develop the relationship between the fractal dimension and hydrology parameters, because fractal have potential as a descriptive tool for scaling up various scales.

References

[1] Feder J. *Fractals*. Plenum Press, New York, 1988.
[2] Bloschl G, Sivapalan M. Scale issues in hydrological modelling: A review. In Kalma JD, Sivapalan M, editors, Scale issues in hydrological modelling, *Advances in Hydrological Processes*, 1995.
[3] Mandelbrot BB. *The Fractal Geometry of the Nature*. Freeman, San Francisco, 1983.
[4] Gimenez D, Allmaras RR, Huggins DR, Nater EA. Prediction of the saturated hydraulic conductivity-porosity dependence using fractals. *Soil Sci. Soc. Am. J.* 1997,**61**:1285-1292.
[5] Baveye P, Pariange JY, Stewart BA. *Fractals in Soil Science. Advances in Soil Science*. CRC Press, 1998.
[6] Rieu, M, Sposito G. Fractal fragmentation, soil porosity, and soil water properties : I. Theory. *Soil Sci. Soc. Am. J.* 1991;**55**:1231-1238.
[7] Perfect E, McLaughlin NB, Kay BD, Topp GC. An improved fractal equation for the soil water retention curve. *Water Res. Res.* 1996;**32**:281-287.
[8] Nielsen DR, Biggar JW, Erh KT. Spatial variability of field-measured soil-water properties. *Hilgardia* 1973;**42:**215-259.
[9] Dagan G. Solute transport in heterogeneous porous formations. *J. Fluid Mech.* 1984;**145**:151-177.
[10] Gelhar LW, Axness CL. Three-dimensional stochastic analysis of macrodispersion in aquifers. *Water Resour. Res.* 1983;**19**:161-180.
[11] Comegna A, Coppola A, Comegna V, Severino G, Sommella A, Vitale CD. State-space approach to evaluate spatial variability of field measure soil water status along a line transect in a volcanic-vesuvian soil. *Hydrol. Earth Syst. Sci*. 2010;**14:**2455-2463.
[12] Coppola A, Comegna A, Dragonetti G, Dyck M, Basile A, Lamaddalena N, Kassab M, Comegna V. Solute transport scales in an unsaturated stony soil. *Adv. Water Resour*. 2011;**34:**747-759.
[13] Severino G, Comegna A, Coppola A, Sommella A, Santini A. Stochastic analysis of a field-scale unsaturated transport experiment. *Adv. Water Resour.* 2010;**33:**1188-1198.
[14] Coppola A, Comegna A, Dragonetti G, Lamaddalena N, Kader AM, Comegna V. Average moisture saturation effects on temporal stability of soil water spatial distribution at field scale. *Soil Till. Res.* 2011;**114**:155-164.
[15] Comegna V, Vitale C. Space-time analysis of water status in a volcanic vesuvian soil. *Geoderma* 1993;**60**:135-158.
[16] Romano N. Use of an inverse method and geostatistics to estimate soil hydraulic conductivity for spatial variability analysis. *Geoderma* 1993;**60**:169-186.
[17 Sudicky EA. A natural gradient experiment on solute transport in a sand aquifer Spatial variability of hydraulic conductivity and its role in the dispersion process. *Water Resour. Res.* 1986;**22**:2069-2082.
[18 Burrough PA. Fractal dimension of landscapes and other environmental data. *Nature*, 1981;**2S4(5838)**:240-242.
[19 Burrough PA. Multiscale sources of spatial variation in soil, I, The application of fractal concepts to nested levels of soil variation. *J. Soil Sci*. 1983a;**34**:577-597.
[20] Burrough PA. Multiscale sources of spatial variation in soil, II, A non-Brownian fractal model and its application in soil survey. **J**.*Soil Sci***.** 1983b;**34**:599-620.
[21] Gajem YM, Warrick AW, Myers DE. Spatial dependence of physical properties of a typical Turrifluvent. *Soil. Soil Sci. Soc. Am. J.* 1981;**45**:1040-1048.
[22] Molz FJ, Liu HH, Szulga J. Fractional Brownian motion and fractional Gaussian noise in subsurface hydrology: a review, presentation of fundamental properties and extensions. *Water Resur. Res*. 1997;**33**:2273-2286.
[23] Molz FJ, Rajaram H, Lu S. Sthocahstic fractal based models of heterogeneity in subsurface hydrology: origins applications, limitations and future research questions. *Rev. Geophys*. 2004;**42(1)**, RG1002.
[24] Hurst HE. A suggested statistical model for some time serials that occur in nature. *Nature* 1957;**280:**494-495.
[25] Mandelbrot BB, Wallis JR. Computer experiments with fractional Gaussian noises I-III. *Water Resour. Res.* 1969;**5:**228-267.
[26] Mandelbrot BB. A fast fractional Gaussian noise generator. *Water Resour. Res.* 1971;**7**:545-553.
[27] Orey S, Gaussian sample functions of the Hausdorff dimension of level crossing. Zaitschrift fur Wahrscheinlichkeits-*Theorie und verwante Gebiete* 1970;**15**:249-256.
[28] Barry M, Lewis ZV. On the Weierstrass-Mandelbrot fractal functions. *Proc. Roy. Soc.* 1980;**370**:459-484.
[29] Turcotte DL. *Fractals and Chaos in Geology and Geophisics*. Cambridge Univ. Press., Cambridge, 1992.
[30] Borrough PA. Soil variability. *Soil and Fertilizers* 1994;**56**:529-562.